Nanosecond Pulse Generation with Silver Nanoparticle Saturable Absorber *

R. Z. R. R. Rosdin[1], M. T. Ahmad[1], A. R. Muhammad[1], Z. Jusoh[2], H. Arof[1], S. W. Harun[1,3]**

[1]*Photonics Engineering Laboratory, Department of Electrical Engineering, University of Malaya, Kuala Lumpur 50603, Malaysia*

[2]*Faculty of Electrical Engineering, Universiti Teknologi Mara (Terengganu), Dungun 23000, Malaysia*

[3]*Department of Physics, Faculty of Science and Technology, Airlangga University, Surabaya, Indonesia*

(Received 6 January 2019)

Nanosecond pulse generation in an erbium-doped fiber laser (EDFL) passively mode-locked by a silver nanoparticle (SNP)-based saturable absorber (SA) is experimentally demonstrated. The SA is fabricated by depositing a nanosized SNP layer onto the surface of polyvinyl alcohol film through the thermal evaporation process. By inserting the SA into an EDFL cavity, stable mode-locked operation is achieved at 1561.5 nm with the maximum pulse energy up to 52.3 nJ. The laser operates at a pulse repetition frequency of 1.0 MHz with a pulse width of 202 ns. These results suggest that SNPs could be developed as an effective SA for mode-locking pulse generation.

PACS: 42.55.Wd, 42.60.Gd, 42.70.Nq DOI: 10.1088/0256-307X/36/5/054202

Nanosecond pulses are normally used to generate high-energy pulsed lasers for potential applications in many areas such as metrology, micromachining, telecommunication and bio-medicine.[1−3] Nanosecond pulsed lasers normally have a low repetition rate in the range of a few MHz and their energies can be easily increased to microjoule levels through external amplification. Conventionally, nanosecond pulsed lasers can be realized through an active technique by incorporating electro-optic or acousto-optic modulators inside a fiber laser cavity, and thus the laser system is bulky with high cost. The nanosecond laser can also be obtained by a passive technique based on Q-switching and mode-locking. Passively Q-switched lasers are normally generated by employing a crystal-based passive saturable absorber (SA), such as Cr:YAG, as a Q-switcher. However, it is difficult to achieve a stable pulse train by this approach. On the other hand, stable nanosecond pulses can be obtained by extension of the cavity length in a passively mode-locked fiber laser using the nonlinear polarization rotation (NPR) technique[4,5] or semiconductor saturable absorber mirror (SESAM).[6] However, NPR-based mode-locked fiber lasers require the adjustment of the polarization state of the oscillating light in the cavity. Therefore, they are relatively disadvantageous in terms of reliability and environmental stability. SESAMs are widely used, but they are still quite costly for the purposes of mass production.

Recently, two-dimensional (2D) nanomaterials such as graphene, black phosphorus, transition metal dichalcoganides and topological insulators have caused great interest for SA applications.[7−9] Most of these works focused on obtaining Q-switching pulses with microsecond pulse width and mode-locking pulses with femtosecond or picosecond pulse width. Only a few works have been reported to generate nanosecond pulses. For instance, Xu *et al.* demonstrated a mode-locked nanosecond erbium-doped fiber laser (EDFL) using a graphene SA.[10]

On the other hand, despite the fact that many new materials and techniques have been found to develop new SAs for Q-switching and mode-locking pulse generations, metal nanoparticle-based materials are rarely investigated. Metal nanoparticles such as gold and silver nanoparticles (SNPs) have garnered great interest from scientific researchers because of their unique optical properties such as large third-order nonlinearity, broadband surface plasmon resonance absorption and fast response time.[11−14] Recently, Wu *et al.* demonstrated a Q-switched laser with a copper nanowire SA. In another work, Hao *et al.* demonstrated a self-started Q-switched fiber laser operating in the C-band region using an SNP-based SA. The SNPs were deposited at the end of a fiber ferrule using a photo-deposition technique to create a fiber-compatible SA with a modulation depth of 18.5%.[11]

In this Letter, we report the use of an SNP thin film-based SA to generate stable nanosecond pulses from an EDFL in a long ring cavity. The SA was obtained by depositing nanosized particles of silver onto the surface of polyvinyl alcohol (PVA) film through the thermal evaporation process. The SA was sandwiched between two fiber ferrules, which offer simplicity, flexibility and easy integration into the laser cavity. The results show a train of self-started mode-locking pulses with a pulse width of 202 ns and a repetition rate of 1.0 MHz. The proposed mode-locked laser operates at 1561.5 nm which is desirable for optical communications and other applications that require all-fibers.

In the experiment, pure silver pallets were used as the SA material while the water-soluble synthetic polymer, i.e., PVA, was prepared in the form of thin film as a host material. The PVA thin film was se-

*Supported by the Ministry of Higher Education Grant Scheme of Malaysia under Grant No PRGS/1/2017/STG02/UITM/02/1.

**Corresponding author. Email: swharun@um.edu.my

© 2019 Chinese Physical Society and IOP Publishing Ltd

lected because it has a low optical absorption at a wavelength of 1560 nm. In addition, PVA has a high flexibility, high strength and is easy to integrate onto the fiber ferrule. Before depositing the SNPs onto the PVA thin film, a pure PVA film was prepared by dissolving 1 g PVA powder (40000 MW, Sigma Aldrich) into 120 ml DI water. With the aid of heat at 145℃, the mixture was stirred until the powders were completely dissolved. Then, 5 ml PVA solution was carefully poured into a petri dish and left to dry under ambient conditions for 3 days to obtain a 50 μm thin layer film. Silver film was deposited onto the surface PVA thin film inside the thermal evaporation chamber of an electron beam machine (KENOSISTEC E-beam). The machine was operated at a vacuum pressure of 10^{-6} Torr inside the chamber. Current was applied to the tungsten filament in the chamber to produce an emission of electrons that beamed onto the silver pallets. During the deposition process, the silver pallets were intensely heated by the Joule effect until they evaporated to produce nanoparticles of silver, which were deposited onto the film surface. The thickness of the silver layer was pre-set at 16 nm. The fabricated SNP film was kept and sealed in a vacuum bag, and placed in a humidity cabinet to prevent the oxidation of silver. An illustration of the preparation process is shown in Fig. 1.

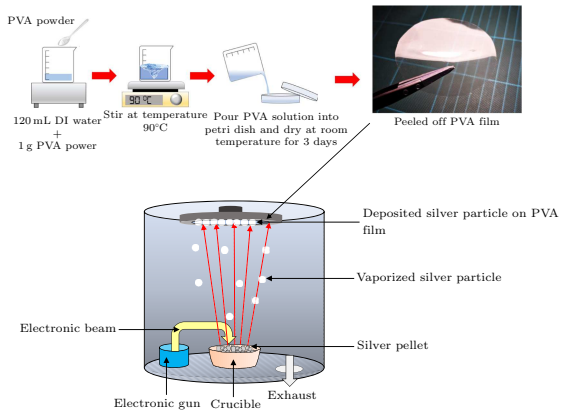

Fig. 1. Fabrication process of the SNP SA thin film.

The fabricated SNP film was analyzed using the energy-dispersive x-ray (EDX) method to identify the existence of the silver element. The result is shown in Fig. 2(a). The resulting spectrum reveals that C, O and Ag elements are present in the SA film. C is the most abundant as it forms the base material of the PVA thin film $(C_2H_4O)_x$. It was also found that about 85.99 Wt% of Ag or silver element exists on the surface of the PVA film. Figure 2(b) shows an image of the SNPs deposited on the PVA film. In addition, the surface morphology of SNPs on PVA was also characterized using focused ion beam scanning electron microscopy (FiB-SEM) at a magnification of 40000× as shown in the inset figure. It is shown that the high density of SNPs was homogeneously distributed onto the PVA film without any aggregation. The average diameter of the SNPs was measured to be around 50 nm. The absorption property of the SNP film was also investigated and the result is illustrated in Fig. 2(c) within a wavelength region from 1450 to 1850 nm with consideration of the measured 7 dB insertion loss. As shown in the figure, the absorption loss is about 1 dB in the 1550 nm region. The modulation depth of the developed SNP film is 19% with a saturation intensity of 170.26 mW/cm^2.

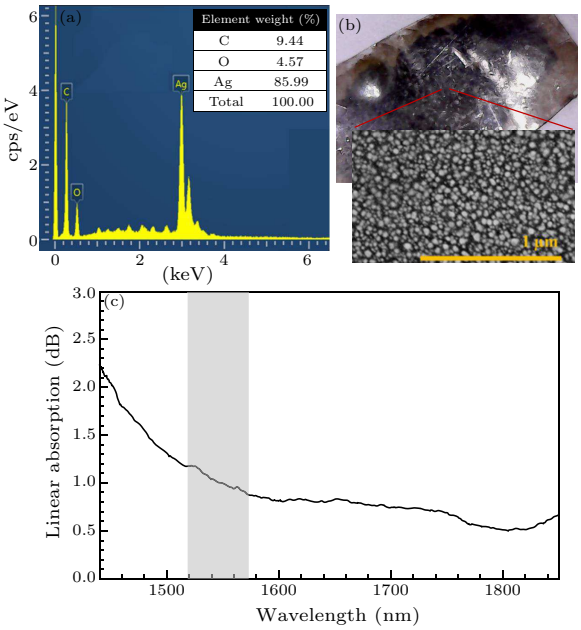

Fig. 2. (a) EDS spectrum of the SNP PVA film. (b) Image of SNPs deposited on the PVA film. Inset shows the surface image of SNP SA using FiB-SEM at magnification of 40000×. (c) Absorption spectrum in the highlighted C-band region.

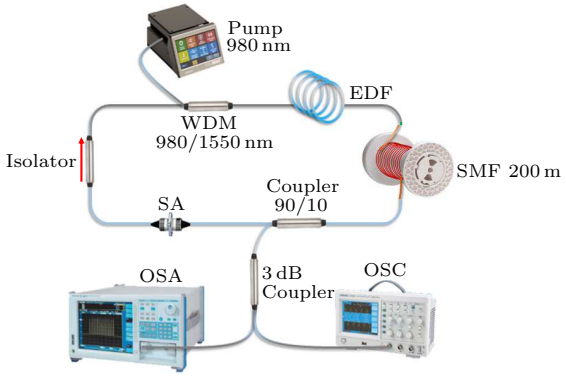

Fig. 3. Schematic diagram of the Q-switched EDFL configuration.

Figure 3 shows the schematic diagram of the proposed nanosecond laser based on the EDFL cavity. The laser cavity is based on a ring configuration and consists of a 2-m-long erbium-doped fiber (EDF) as the gain medium, a 200-m-long standard single mode fiber (SMF), a 90/10 output coupler, an isolator, a 980/1550 nm wavelength division multiplexer (WDM), and a newly developed SNP thin film-based SA. The EDF has a pump absorption rate of about

14.5 dB/m at 980 nm. It was forward-pumped by a 980-nm pump via the WDM. The isolator was incorporated inside the laser cavity to ensure unidirectional propagation of light and thus preventing any detrimental effects inside the laser resonator. The SA device was constructed by sandwiching a tiny piece of the prepared SNP film between two fiber ferrules via a fiber adapter to form a fiber-compatible device. A small amount of index-matching gel was used at the connection to minimize parasitic reflections. The insertion loss of the SA device was recorded as 5.5 dB at 1560 nm. The 200-m-long SMF was added into the cavity to tailor the dispersion characteristics and nonlinearity of the cavity and allow a nanosecond pulse generation. The output coupler was used to tap out 10% of the output for observation and retain 90% to oscillate in the cavity. An optical spectrum analyzer (OSA) with a spectral resolution of 0.05 nm was used to observe the optical spectrum of the mode-locked EDFL, while a 500 MHz digital oscilloscope was used to analyze the output pulse train via a photodetector. The optical power meter was swapped with an OSA to measure the average output power of the laser output. A 7.8 GHz rf spectrum analyzer was used to investigate the repetition rate and stability of the laser. The overall length of the laser cavity was approximately 211 m.

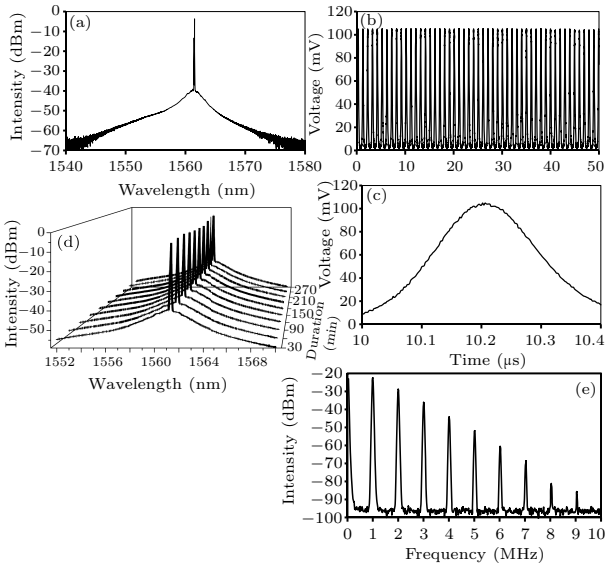

Fig. 4. Mode-locking performance of the output pulse train: (a) output spectrum, (b) typical pulse train operating at 1.0 MHz, (c) corresponding single-pulse envelope showing the pulse width of 202 ns, (d) output spectra evolution for 5 h duration of operation, and (e) rf spectrum.

The performance of the proposed SNP-based EDFL was investigated by varying the power of the 980 nm pump. A stable self-started mode-locked pulse was obtained when the 980 nm pump power was increased gradually above the threshold of 198.0 mW. This mode-locking threshold is relatively high due to the high insertion loss of the film SA and long cavity. The mode-locking operation was also observed to remain stable as the pump power was further increased to the maximum available pump power of 223.4 mW. Figure 4(a) shows the output optical spectrum at the threshold pump power, operated at 1561.5 nm. The narrow optical spectral bandwidth of the mode-locked laser indicates that the mode-locking pulse train is working in a relatively large spectral duration (nanosecond regime). Figure 4(b) shows the oscilloscope trace of the mode-locked pulse train at the threshold pump power. The time interval between the pulses is about 1 μs, which matches with the cavity length of 211 m. The pulse width of the laser was kept at around 202 ns when adjusting the value of pump power from 198.0 to 223.4 mW. Figure 4(c) illustrates the single pulse envelope of the oscilloscope trace, which has a full width at half maximum of 202 ns. To investigate the laser stability of the mode-locking operation, the laser spectrum was recorded every 30 min for 5 h. As shown in Fig. 4(d), stable operation centered at 1561.5 nm wavelength with peak amplitude variation within ±1 dB was observed. The stability of the laser was further investigated based on the rf spectrum, which was obtained using an rf spectrum analyzer. The result is plotted in Fig. 4(e) at the threshold pump power of 198.0 mW. It indicates a fundamental frequency of 1.0 MHz with nine harmonics. This frequency matches very well with the peak-to-peak duration (pulse period) of the oscilloscope trace. The obtained rf spectrum has a high signal-to-noise ratio (SNR) of up to 74.3 dB, further indicating the excellent stability of the pulses. To verify that the SNP material was responsible for the laser's mode-locking pulse generation, the SNP PVA film was replaced with pristine PVA film in the setup. In this case, no mode-locking pulses were visible on the oscilloscope at any pump power. This confirms that the mode-locking operation was attributed to the SNP SA. Oxidation of the silver film in this work shows no significant effect on the long-term stability of the mode-locking operation, which was supported by the 5-hour run of the stability test as shown in Fig. 4(d). It is also worth noting that the Q-switching operation could be easily achieved by removing the 200-m-long SMF from the laser cavity.

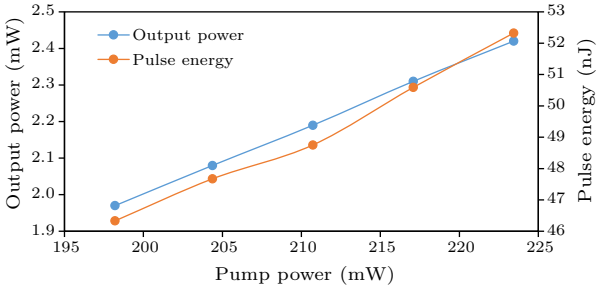

Fig. 5. Average output power and pulse energy against pump power.

Figure 5 shows the mode-locked output power and single pulse energy against the input pump power. As

shown in the figure, the output power increases from 1.97 mW to 2.42 mW with the corresponding pump power input from 198.0 mW to 223.4 mW. The slope efficiency from the graph is calculated to be 1.78%, which is relatively low due to the high insertion loss from the SA. From the graph, it is also observed that the maximum pulse energy of 52.3 nJ is achieved and the pulse energy increases linearly with the pump power. The performance of this laser is comparable with other SA-based lasers. However, this laser is expected to have a higher optical damage threshold for mode-locking applications. The performance of mode-locked pulses including the threshold pump power is expected to be further improved by optimization of both SA parameters and the laser cavity design. The SNP SA loss can be improved by reducing the thickness of the PVA film and the SNP layer. A thinner SNP layer may reduce the scattering loss. These results verify the mode-locking ability and show that the SNP material could be used in optoelectronic devices and communication devices in the C-band region.

The performance of the SNP thin film as compared to SAs based on other real SA materials is given in Table 1. As shown in the table, the laser performance is comparable with other SAs. It is also observed that a high SNR value and a high maximum pulse energy output are achieved by integrating the proposed SA. In this work, the PVA film functions to hold the SNP so that it can easily be incorporated into a laser setup and it is not involved in the mode-locking operation. However, the saturable absorption effect can also be induced by PVA due to O–H bond absorption in a certain wavelength region outside the erbium gain spectrum. Further study should also be focused on obtaining the Q-switching and mode-locking pulse trains in the O–H absorption region.

Table 1. Comparison of typical mode-locked pulsed laser with different SA materials. RR: repetition rate.

SA material	RR (MHz)	Cavity length (m)	Pulse energy (nJ)	Output power (mW)	SNR (dB)	
SNP	∼1.0	211	52.3	1.97–2.42	74.3	This work
V_2O_5	∼1.0	201	4.44	2.91–4.72	48.58	Ref. [15]
Sb_2Te_3	∼3.75	54	0.133	∼65	55	Ref. [16]
BP	1.843	112.4		0.12–4.43	54	Ref. [17]

In conclusion, a stable all-fiber passively mode-locked EDFL generating a nanosecond pulse train has been successfully demonstrated using an SNP-based SA. The SA used in our experiment was prepared by depositing nanosized silver particles onto the surface of PVA film through the thermal evaporation process. By incorporating the SA into the laser cavity, stable mode-locked nanosecond pulses at 1561.5 nm with a pulse duration of 202 ns and a fundamental repetition rate of 1.0 MHz were obtained. The average output power was 2.42 mW, corresponding to a single pulse energy of 52.3 nJ at a pump power of 223.4 mW. The fundamental frequency of the rf spectrum shows an SNR of 74.3 dB, indicating the excellent stability of the pulses. The experimental results suggest that SNPs are a promising material for ultrafast light generation in the C-band region.

References

[1] Dornfeld D, Min S and Takeuchi Y 2006 *CIRP Ann.* **55** 745
[2] Clowes J 2008 *Opt. Photonik* **3** 36
[3] Luo L G, Chu P L and Liu H F 2000 *IEEE Photon. Technol. Lett.* **12** 269
[4] Mao D, Liu X M, Wang L R, Hu X H and Lu H 2011 *Laser Phys. Lett.* **8** 134
[5] Mao D, Liu X, Wang L, Lu H and Feng H 2010 *Opt. Express* **18** 23024
[6] Chen L, Zhang M, Zhou C, Cai Y, Ren L and Zhang Z 2009 *Electron. Lett.* **45** 731
[7] Bao Q, Zhang H, Wang Y, Ni Z, Yan Y, Shen Z X, Loh K P and Tang D Y 2009 *Adv. Funct. Mater.* **19** 3077
[8] Hisyam M B, Rusdi M F M, Latiff A A and Harun S W 2017 *IEEE J. Sel. Top. Quantum Electron.* **23** 39
[9] Yan P, Lin R, Ruan S, Liu A, Chen H, Zheng Y, Chen S, Guo C and Hu J 2015 *Sci. Rep.* **5** 8690
[10] Xu J, Wu S, Liu J, Wang Q, Yang Q H and Wang P 2012 *Opt. Commun.* **285** 4466
[11] Guo H, Feng M, Song F, Li H, Ren A, Wei X, Li Y, Xu X and Tian J 2016 *IEEE Photon. Technol. Lett.* **28** 135
[12] Wu D, Peng J, Cai Z, Weng J, Luo Z, Chen N and Xu H 2015 *Opt. Express* **23** 24071
[13] Glubokov D A E, Sychev V V E, Mikhailov A S, Korolkov A E E, Chubich D A E, Shapiro B I and Vitukhnovskii A G E 2014 *Quantum Electron.* **44** 314
[14] Varnavski O P, Goodson III T, Mohamed M B and El-Sayed M A 2005 *Phys. Rev. B* **72** 235405
[15] Nady A, Baharom M F, Latiff A A and Harun S W 2018 *Chin. Phys. Lett.* **35** 044204
[16] Sotor J, Sobon G, Macherzynski W and Abramski K M 2014 *Laser Phys. Lett.* **11** 055102
[17] Chen Y, Mu H, Li P, Lin S, Nanjunda S B and Bao Q 2016 *Opt. Eng.* **55** 081317